Available online at www.sciencedirect.com
ScienceDirect
Polymer 49 (2008) 278–294
polymer
www.elsevier.com/locate/polymer

Miscibility, morphology, thermal, and mechanical properties of a DGEBA based epoxy resin toughened with a liquid rubber

Raju Thomas [a], Ding Yumei [b], He Yuelong [b], Yang Le [c], Paula Moldenaers [d], Yang Weimin [b], Tibor Czigany [e], Sabu Thomas [f,*]

[a] Department of Chemistry, Mar Thoma College, Tiruvalla 689 103, Kerala, India
[b] College of Mechanical and Electrical Engineering, Beijing University of Chemical Technology, Beijing 100029, PR China
[c] College of Materials Science and Engineering, Beijing University of Chemical Technology, Beijing 100029, PR China
[d] Department of Chemical Engineering, K.U. Leuven, de Croylaan 46, B-3001 Leuven, Belgium
[e] Budapest University of Technology and Economics, Faculty of Mechanical Engineering, Department of Polymer Engineering, H-1111 Budapest, Muegyetem rkp.3. T. bld.111. 33, Hungary
[f] School of Chemical Sciences, Mahatma Gandhi University, Priyadarshini Hills P.O., Kottayam 686 560, Kerala, India

Received 22 April 2007; received in revised form 26 October 2007; accepted 6 November 2007
Available online 19 November 2007

Abstract

Epoxy resin based on diglycidyl ether of bisphenol A and varying content of hydroxyl terminated polybutadiene were cured using an anhydride hardener. The ultimate aim of the study was to modify the brittle epoxy matrix by liquid rubber to improve the toughness characteristics. Chemorheological analysis of the modified network was performed to understand the physical transformations taking place during the cure polymerization reaction. The delay in gel time on inclusion of rubber can be explained by lower reactivity due to dilution and viscosity effect. Tensile, flexural, and fracture toughness behaviors of neat as well as modified networks have been studied to observe the effect of rubber modification. The morphological evolution of the toughened networks was examined by scanning electron microscope, and the observations were used effectively to explain the impact properties of the network having varying content of liquid rubber. Acoustic emission studies were performed on neat and certain modified systems. Based on acoustic emission results and morphological characteristics, toughening and failure mechanisms were discussed. The behavior of the relaxation peaks were evaluated by dynamic mechanical analysis and tried to explain the composition of networks. Thermal stabilities of the toughened epoxies were studied using thermogravimetric analysis (TGA). The activation energy for decomposition of neat and modified epoxies has been estimated and compared. The reduction in cross-linking density of the thermoset upon modification has been confirmed and explained.

Keywords: Epoxy resin/liquid rubber; DSC; Mechanical properties

1. Introduction

Epoxy resins are characterized with outstanding performances such as toughness, rigidity, high temperature performance, chemical resistance, adhesive properties, formulation latitude, and reactivity with a wide variety of chemical curing agents [1]. The resin forms a highly cross-linked network structure having relatively high stiffness and glass transition temperature (T_g) with high chemical resistance. However, the inherent toughness of the network polymer is low. Elastomeric modification is one of the most frequently used and widely accepted methods for improving properties of epoxy networks. The copolymer of acrylonitrile and butadiene with end carboxyl functional groups, CTBN, can react with the epoxide groups, and hence are popularly employed as a modifier to epoxy. A high level of interfacial adhesion and property improvements are achieved by this elastomer [2–4]. Hydroxyl

* Corresponding author. Tel.: +91 481 2730003; fax: +91 481 2561190.
E-mail addresses: czigany@eik.bme.hu, czigany@pt.bme.hu (T. Czigany), sabut@sancharnet.in, sabut552001@yahoo.com (S. Thomas).
URL: http://www.pt.bme.hu

0032-3861/$ - see front matter © 2007 Elsevier Ltd. All rights reserved.
doi:10.1016/j.polymer.2007.11.030

terminated internally epoxidized polybutadiene rubber has been used as a modifier for epoxy matrix in a number of studies [5–7]. Barcia et al. [8] employed HTPB as a surface modifier in carbon fiber (CF) reinforced, epoxy matrix composites. The surfaces of carbon fibers (CFs) were grafted with HTPB, and this formed a flexible interface between CF and epoxy matrix, which ultimately improved the mechanical behavior of the system. In an interesting study, the DGEBA based epoxy resin was modified with block copolymers from isocyanate terminated polybutadiene [9]. Ozturk et al. [10] employed modified HTPB rubbers to improve thermal and mechanical properties and ultimately to toughen an epoxy thermoset matrix.

The objectives of the present study are to investigate the mechanical and fracture behavior of epoxy resin modified with hydroxyl terminated polybutadiene (HTPB) liquid rubber and thus to characterize their morphology and toughening mechanisms. The obvious characteristic of the elastomer is its immiscible nature with the epoxy resin and hence in a phase separated state from the major epoxy matrix throughout the cure reaction. In the literature there are not many works on the structure–property relationship of epoxy–HTPB system. The importance of the study is that a cyclic anhydride is used as a curing agent. Based on the mechanical properties and morphological analysis, attempts have been made, to analyze toughening mechanisms prevailing in the phase separated matrix. Since the composition varies, chemical reaction kinetics and hence cross-linking nature of cured product alter which lead to variations in mechanical behavior. Analysis of the structure–property relationship of epoxy–cyclic anhydride–HTPB system is a new endeavor to the best of our knowledge. Based on acoustic emission studies and morphology, a failure mechanism has been proposed. Viscoelastic properties and thermal analyses of modified epoxies have been studied. Decrease in cross-link density was observed with the inclusion of elastomer.

2. Experimental

2.1. Materials

The epoxy resin used was liquid diglycidyl ether of bisphenol A (DGEBA) (Araldite Gy 250) with an equivalent value of 5.3 eq kg^{-1}. An anhydride (under the trade name, Hy 906) was used as curative. *N*,*N*-Dimethyl benzylamine was used as the accelerator having the trade name of Gy-062. All the chemicals were supplied by Huntsmann, Mumbai, India. The liquid rubber, hydroxyl terminated polybutadiene HTPB, was supplied by Vikram Sarabhai Space Center, India. Fig. 1 shows the structures of components and Table 1 gives the characteristics of HTPB.

2.2. Preparation of epoxy–HTPB blend

Stoichiometric amount of epoxy resin and hardener were taken and stirred for 10 min to ensure proper dispersion of hardener. Varying weights of HTPB were added followed by accelerator and stirred again for 15 min. The system was degassed to remove any issuing gases for 5 min and poured into a steel mould, which was greased. The sample was then pre-cured at 100 °C for 30 min followed by post curing for 1.5 h at 180 °C. The cure condition was chosen from DSC studies performed in the dynamic mode, which revealed that almost all curing process took place before 180 °C. Fig. 2(a) demonstrates the dynamic DSC curve of 10 phr epoxy–HTPB blend.

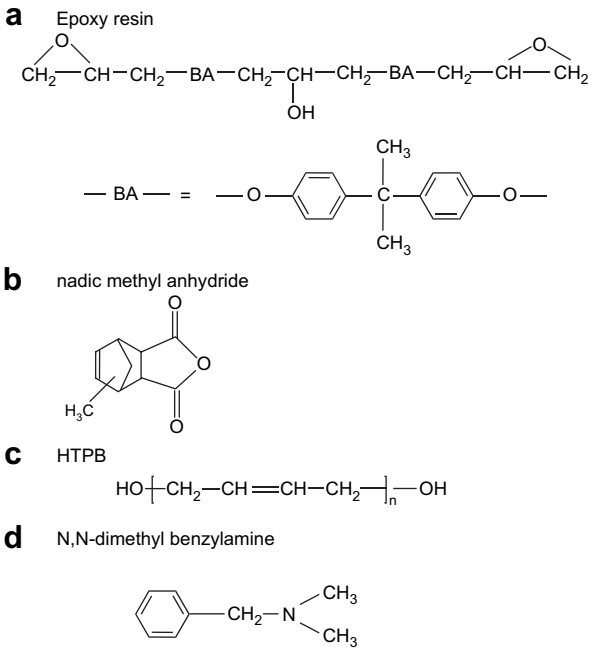

Fig. 1. Structure of compounds.

2.3. Characterization

2.3.1. Differential scanning calorimetry (DSC)

Differential scanning calorimetry (DSC) was performed using Perkin–Elmer DSC-7 equipment, USA. The cure conditions were determined in the dynamic mode at 5 °C/min (in a dry nitrogen atmosphere and calibrated with an Indium standard) to verify the time to complete the cure process. Isothermal measurements were also done at 100, 120, 140, 160 and 180 °C to calculate the enthalpy related to the curing process. About 3–5 mg of samples in aluminum pans were used for each measurement. The heat evolved during the reaction of the mixture was directly determined by integration of the exothermic peaks. The curves, obtained with the long-time isothermal scanning, were used to determine the degree of conversion and rate of curing using the traditional procedure of the measurement of the reaction heat [11,12].

Table 1
Characteristics of HTPB liquid rubber

Hydroxyl value (mg KOH g^{-1})	42.4
Acid value (mg KOH g^{-1})	0.3
Specific gravity at 25 °C	0.9055
Molecular weight (VPO)	2710
Viscosity at 30 °C, Brookfield (cps)	6160

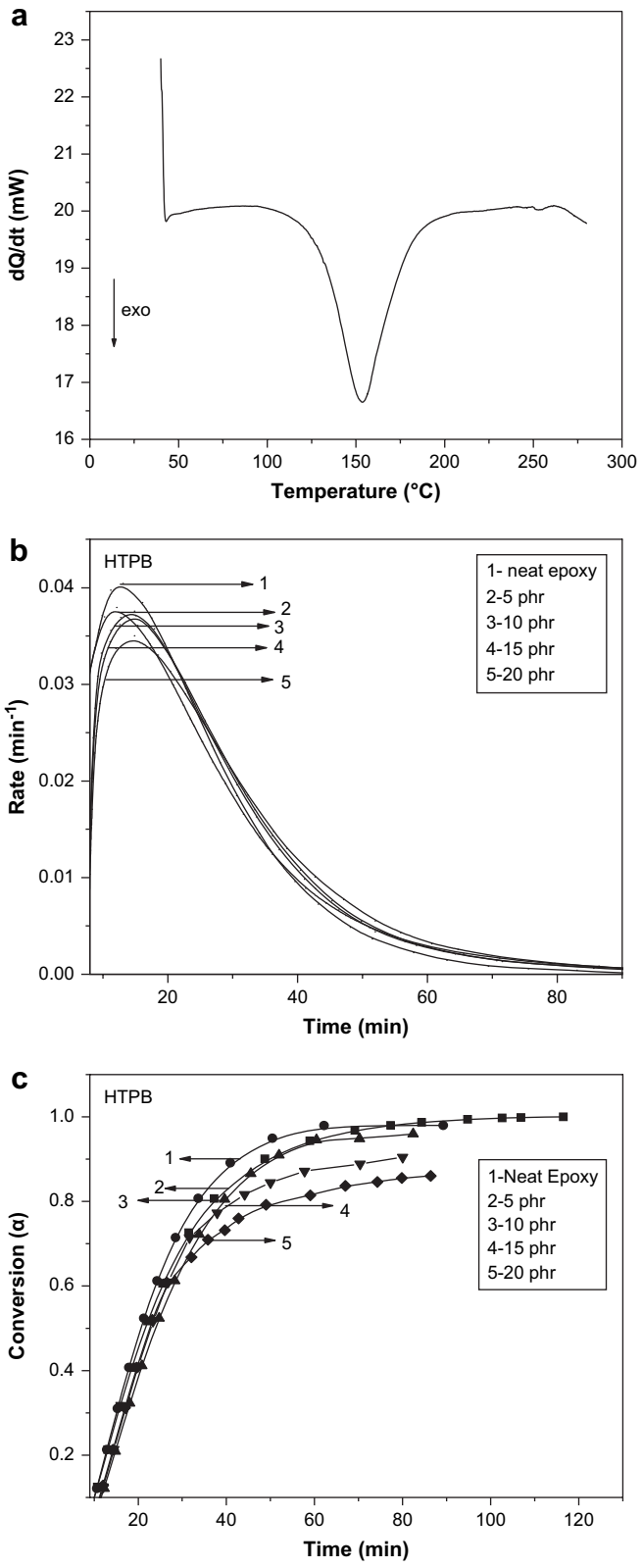

Fig. 2. (a) Dynamic DSC curve of 10 phr epoxy–HTPB blend. (b) Rate versus time for neat and modified epoxies at an isothermal cure temperature of 120 °C. (c) Conversion versus time for neat and modified epoxies at an isothermal cure temperature of 120 °C.

2.3.2. Determination of gel point

The gel point was determined according to ASTM 2471, by putting about 100 mg of the sample in several tubes, which were placed into an oil bath at 100 °C. The tubes were withdrawn from the bath at different times and chilled in an ice bath to quench the reaction. The polymeric material was dissolved with tetrahydrofuran (THF). The gelation point was determined from the presence of insoluble fraction.

2.3.3. Rheological analysis

Rheological dynamic time sweeps were performed by a Dynamic stress controlled Rheometer in the laboratory of Department of Chemical Engineering, K.U. Leuven, Belgium to study the variations of rheological properties during cure. Parallel plate geometry (25 mm diameter) under a constant stress of 50 Pa was used in the oscillatory mode at a constant frequency of 1 Hz keeping a strain of 5%. All measurements were done at N_2 atmosphere. Gelation was defined as the point where the loss factor ($\tan\delta$) becomes independent of frequency [13,14]. Viscosities of the modified resins were also recorded by the same instrument.

2.3.4. Morphology analysis

Scanning electron micrograph (SEM) was performed using a JEOL JSM 5800 model SEM, Belgium with an electron voltage of 15 kV and secondary electron detector to examine the fracture surfaces of toughened epoxy matrices. The samples were fractured under liquid nitrogen and first treated with toluene to extract the rubber phase, then dried under vacuum. A thin section of the fractured surface was cut and sputter coated with a thin layer of gold prior to fractographic analyses. The size and distribution of dispersed particles were determined by means of semiautomatic image analyses. The SEM micrograph of the fractured surface was first scanned and converted into digitized image, which was analyzed using an ''Analysis 3.0'' programme to obtain the average diameter values of the dispersed particles and particles size distribution.

2.3.5. Mechanical testing

The tensile tests were also performed in an Instron 4204 testing machine, India, at a crosshead speed of 1 mm/min, according to ASTM D-638. The specimens were cut from cured sheets using a fine band saw to dimensions of $85 \times 20 \times 3$ mm^3. The values were taken from an average of at least five specimens.

Fracture toughness, K_{IC}, measurement was done on single-edge notched SEN-T specimens cut from the plates of epoxy–liquid elastomer blends. The dimensions of the specimens were in the following order: length = 110 mm, breadth = 30 mm, thickness = 3 mm, and length of notch = 10 mm. Before the measurement the cuts were made sharper by sawing and sharpening with a razor blade.

Fracture toughness was determined from the load–displacement curve when the loading is increased monotonously. (Tensile tester ZWICK Z020 universal testing machine, Hungary at 1 mm/min crosshead speed at room temperature.)

From the load–elongation response of the SEN-T specimens the fracture toughness can be determined using the following expression:

$$K_{IC} = \frac{F_{max}}{BW} a^{1/2} f\left(\frac{a}{W}\right) \quad (1)$$

where F_{max} = maximum force from the load–elongation trace; B = thickness of the specimen; W = width of the specimen; a = total notch length (produced by saw and razor blade).

$f(a/W)$is the geometry correction factor and is expressed as:

$$f\left(\frac{a}{W}\right) = 1.99 - 0.41\left(\frac{a}{W}\right) + 18.7\left(\frac{a}{W}\right)^2 - 38.48\left(\frac{a}{W}\right)^3 + 53.85\left(\frac{a}{W}\right)^4 \quad (2)$$

To evaluate the K_{IC} value, specimen size parameters were determined on each individual specimen.

Critical strain energy release rate (fracture energy) G_{IC} was computed using the expression,

$$G_{IC} = \left(\frac{K_{IC}^2}{E}\right) \quad (3)$$

where E = elastic modulus.

The impact strength of the notched specimens was determined by Charpy Monsanto Tensiometer, China, using rectangular specimens of $60 \times 12 \times 2$ mm^3 according to ASTM standard D 6110-06, 2003. Each specimen was then milled using a Clarkson deadlock facing cutter and notched to a depth of 5.5 mm with a metal slitting saw at an angle of 60° using a Schaublin 53 milling machine. The impact test was carried out at room temperature and the impact energy was reported in Joules per meter. The values were taken from an average of at least ten specimens.

Flexural tests were performed with rectangular samples according to ASTM D-790 using an Instron 4204 testing machine, China fitted with a three-point bending fixture at a crosshead speed of 2 mm/min. The dimensions of the samples were $120 \times 25 \times 2.5$ mm^3 and the span to thickness ratio was set at $L/D = 32{:}1$ in all cases. The flexural strength (FS) was determined from the following formula:

$$FS = \frac{3}{2} \times \text{peakload} \times \text{span} \times \frac{9.8}{\text{width}} \times (\text{thickness})^2 \quad (4)$$

The results are expressed in Mega Pascal (MPa), which is the average of the results from five samples. The flexural strain was also determined.

2.3.6. Acoustic emission studies (AE)

Acoustic emission (AE) measurements were carried out during the tensile test of the SEN-T specimens according to ISO 527 on a computer controlled universal tensile tester type Zwick Z020 at room temperature at 5 mm/min extension speed. The acoustic signals were recorded with a microphone type A-11 that operates based on the piezoelectric principle (Micro30S, Physical Acoustic Corporation, USA) and which was connected to a 16-channel device type, SENSOPHONE AED-40/12 Gereb & Co. Ltd, Hungary, through a logarithmic amplifier. The examinations of the pressed specimens were completed on the same machines with the same parameters and the processes were recorded with a video extensometer and a video camera.

2.3.7. Dynamic mechanical thermal analysis (DMTA)

The dynamic mechanical measurements were performed using a dynamic mechanical analyzer DMA (TA INSTRUMENTS MODEL 2960, Germany). The analysis was carried out from −100 to 250 °C at a heating rate of 3 °C/min, with a fixed frequency of 1 Hz. Dynamic moduli and loss moduli were obtained by dual cantilever mode for the sample of size $60 \times 12 \times 2$ mm^3.

The variation in T_g, as noted from the analysis, can be interpreted in terms of difference in cross-link densities of the matrix [15]. The number average molecular weight between cross-links (M_c) was calculated using the expression [16]:

$$M_c = \frac{3.9 \times 10^4}{T_g - T_{g0}} \quad (5)$$

where T_g = glass transition temperature of cross-linked epoxy resin and T_{g0} = glass transition temperature of uncross-linked polymer having the same composition as the cross-linked polymer.

Effective cross-link density was calculated from M_c using the following equation [17]:

$$\upsilon_e = \frac{\rho N_A}{M_c} \quad (6)$$

where ρ = density and N_A = Avogadro's number.

2.3.8. Thermogravimetric analysis (TGA)

Thermogravimetric analysis was performed with a Du Pont TGA-2950 analyzer, Germany to investigate the thermal resistance of the cured neat and rubber-modified samples. About 10 mg of sample was heated in a platinum crucible from ambient to 850 °C at a heating rate of 10 °C/min. The thermal analysis was done in nitrogen atmosphere (50 mL min^{-1} flow).

3. Results and discussion

3.1. Evaluation of cure parameters and gel point

The effect of HTPB on cure parameters of the cured epoxy network (T_{cure} = 120 °C) is furnished in Table 2. The heat content, ΔH values related to the cure reaction, was measured in an isothermal mode. The values estimated from the area of the exothermic peak at a particular temperature did not change significantly upon the addition of rubber indicating that the presence of rubber has not influenced the mechanism of cross-linking reaction. Gel times which represent the necessary time to produce the minimum amount of insoluble

Table 2
Composition, cure parameters, and gelation times of neat and rubber-modified epoxy systems at 120 °C

Weight percentage of HTPB	ΔH[a] (J/g)	Gelation times (min)			Cure time[a] (min)
		Experiment	Rheology	DSC	
0	208	14	17.5	14.1	33
5	205.4	15	26.6	15.2	36
10	206.2	18	29.1	16.4	38
15	206.5	22	32.0	18.5	40
20	205.9	25	35.0	20.0	43

[a] Obtained from DSC isothermal mode.

fraction was found to be greater for modified epoxies with the addition of rubber and are tabulated in Table 2. This may be attributed to the dilution effect caused by the inclusion of rubber. The result is in agreement with the reported cases in literature, including that of epoxy systems modified with CTBN [18]. However, the results contradict the observation of Barcia et al. [9] in their observations on epoxy systems modified with functionalized polybutadiene where they support a fast reaction attributed to the presence of urethane groups which participate in the curing process. The cure time also increases with the inclusion of the elastomer. This may, again, be due to the effect of dilution. As dilution increases with the addition of the rubber, there will be decrease in the density of the reaction groups [19]. Fig. 2(b) and (c) depicts rate and conversion of the cure polymerization reaction versus time at a cure temperature of 120 °C. From the figures it is clear that the initial rate of reaction and conversion is higher for neat resin, while there is a delay for modified epoxies. The time for the maximum conversion is not the same for all systems as seen from Fig. 2(c). The rate and conversion decrease with the inclusion of rubber, suggestive of the fact that the HTPB rubber does not catalyze the anhydride–DGEBA reaction. The decrease may be attributed to the effect of dilution on the concentration of the reacting species. Alternatively, the retardation in the rate of reaction may be caused by a destabilization of the polar transition state as a result of the reduction in dielectric constant when the less polar rubber is added to the mixture [20].

During the cure polymerization reaction conversion of the reacting groups take place followed by the formation of a three dimensional network of epoxy thermoset. The rubber particles can occupy positions in between the reaction centers thereby separating the cross-linking points. Thus the addition of liquid rubber reduces the cross-linking density of the formed network. There may be changes in the reaction that depend upon the reactivity of the functional groups. The prediction of the exact chemical reaction and the formation and breakage of bonds are difficult to establish. The general reaction pathway for the cure of epoxy resin via tertiary amine catalyst is depicted in Scheme 1. The reaction initiates by the opening

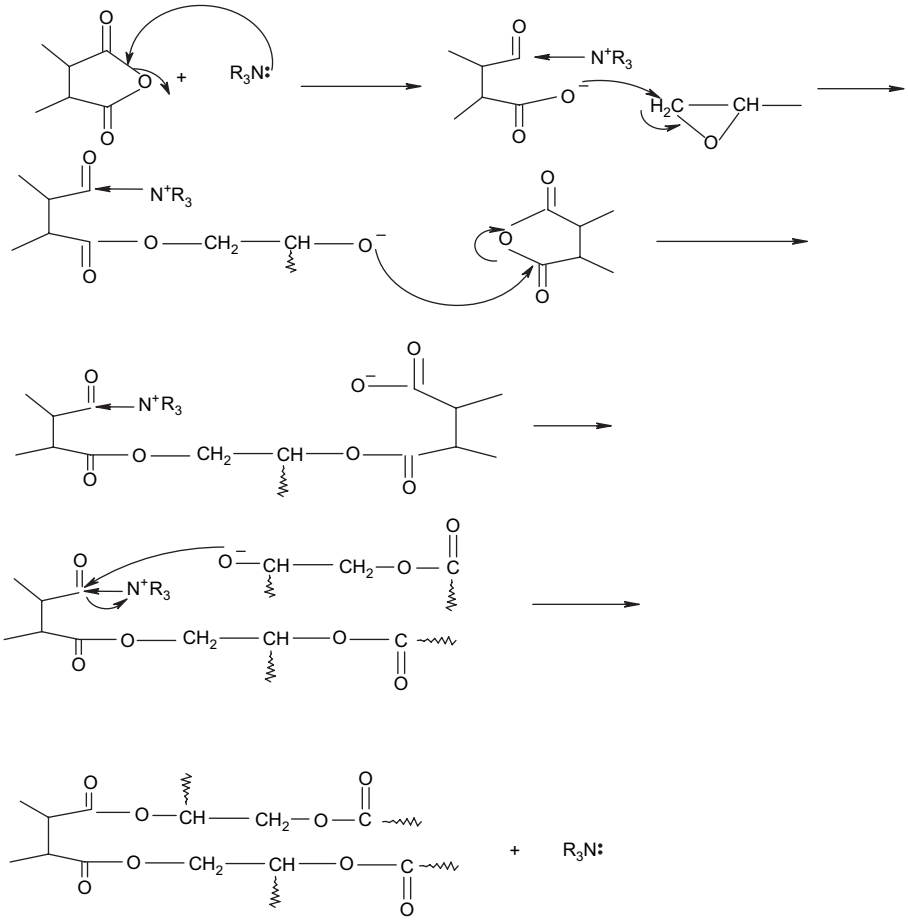

Scheme 1. Cure reaction mechanism of the anhydride and the epoxy resin.

of the anhydride ring with the resultant formation of an anion, which is considered to be a fast reaction. The reaction propagates by the attack of the anion on the epoxy group thereby generating an ester-alkoxide anion, which forms an ester linkage and a second carboxyl anion by reaction with anhydride. The reaction between the anion and the epoxide is considered to be the rate determination step in the reaction scheme.

Kinetic measurements provide a method for the determination of gelation time as per the theory of Flory [21] which defines gelation as the point in which the molecular chain reaches a theoretical infinite molecular weight. Gelation time is considered as point when $\chi_{gel} = 0.36$. The results along with same obtained from rheological analysis are included in Table 2. Rheological gel time will be discussed in the following section. The delay in gel time upon the addition of rubber from DSC may be mainly attributed to the dilution effect and/or viscosity increase because of the rubber addition or by the decrease in the density of reaction groups [19]. Similar observations are reported for thermoplastic-modified epoxy resins [22–25].

3.2. Rheological measurements

Rheological measurements were carried out at different isothermal temperatures to characterize the physical transformations such as gelation and vitrification taking place during curing. Fig. 3(a) depicts the rheological behavior at 120 °C through polymerization of neat epoxy. The curve represents the variation of elastic (G′) and loss modulus (G″) with respect to time for neat resin isothermally cured at 120 °C. Initially the system is in the liquid state having a low stiffness value and hence the elastic modulus is almost constant with varying time. Similarly the loss modulus is also low and constant with varying time. This zone symbolizes the state of the system before the start of curing process. But as curing and resultant cross-linking progresses, both storage and loss moduli increases to have a crossover of G′/G″. This point represents the state of the system where both elastic and viscous behavior prevails, storing a similar amount of energy dissipated. This zone is considered as the occurrence of gelation of the system. G′ exceeded G″ because of the thermoset network formation. Complex viscosity against time for 10 and 15 wt% of rubber-modified epoxies at an isothermal temperature of 120 °C has been plotted, as representative curves, in Fig. 3(b). The small increase in time for attaining a particular viscosity as rubber content varies (which is an indicative of gelation), at a constant temperature, is evident from this figure. It becomes obvious that the chemical reactions are delayed with respect to the inclusion of rubber, supporting the dilution effect. The complete

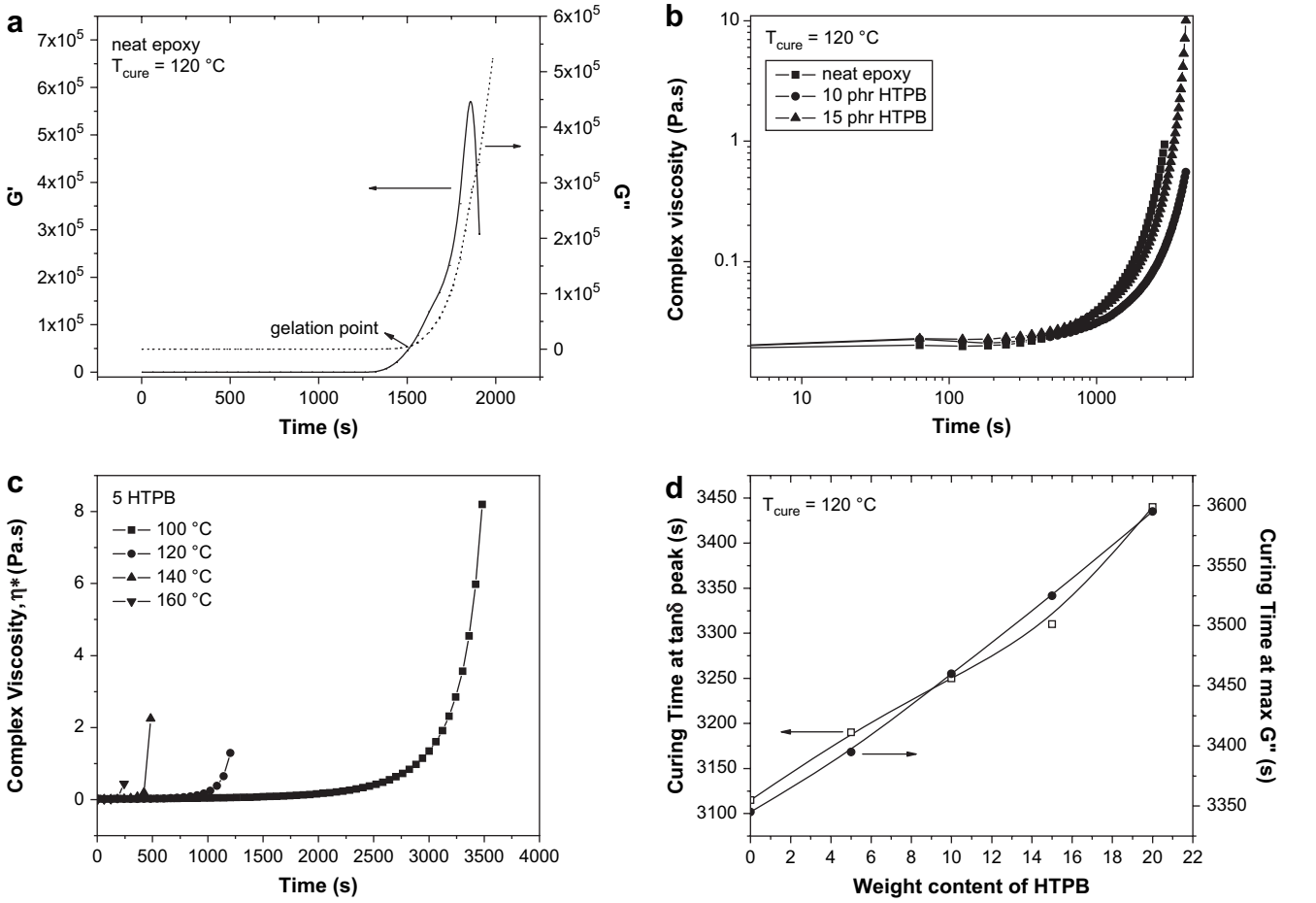

Fig. 3. (a) Rheological curve for neat resin at 120 °C. (b) Complex viscosity versus time for modified blends. (c) Complex viscosities versus time for 10 phr blend at different isothermal cure temperatures. (d) Vitrification times from rheology, $T_{cure} = 120$ °C.

viscosity range could not be attained due to the inbuilt torque of the instrument. Complex viscosity against time for 5 phr rubber concentration has been plotted at different isothermal temperatures, say 100, 120, 140, and 160 °C in Fig. 3(c). With increase in cure temperature the time for attaining gelation state decreases establishing the cure reaction as a thermally catalyzed one. A similar behavior was experienced for all systems. Again, the torque of the instrumentation set up prevents from covering the entire viscosity range of the curing reaction.

Now, the modifier was found to influence the cure reaction and hence the gel time varies. The steady-state viscosity becomes infinite at the gelation point [26,27], which is attributed to the formation of infinite molecular network. However, gelation time is usually taken as the time to attain a finite viscosity in the order of 10^3–10^4 Pa s. [26,28,29]. Table 2 demonstrates rheological and kinetic gelation times at a T_{cure} of 120 °C. It is evident from the table that gel time increases with the increase in the rubber concentration. This delay can be attributed to lower reactivity of the modified epoxy produced as a result of chain extension and increase in viscosity of the medium due to the addition of rubber. As dilution increases with the addition of rubber, the concentration of reacting species gets reduced that impair reactivity. The delay in cure kinetics from rheological studies is well in agreement with the kinetics obtained from thermal measurements. The gelation times obtained from rheological and DSC measurements are not comparable because the values obtained from rheology measurements are larger than that obtained from DSC data. The reasons are attributed due to the difference in sample volume (2–3 g versus 0.005 g), thermal history, and atmosphere used in these techniques [30]. Also, a phase difference between the gelation times from kinetic and rheological measurements are reported by Eloundou et al. [31]. The first reason for this is related to delay in attaining thermal equilibrium when a higher mass of sample is used. The mass of sample used in the rheology study is higher, causing a delay in the onset of kinetics. Catalytic effect of water vapor present in the atmosphere also plays a role. The absorption of water is higher during sample preparation for DSC analysis, as very small amount of sample (0.2–0.5 mg) is used for DSC measurement. No accepted decisive factor has been defined [32] about vitrification. Two different criteria [33] have been adopted to ascertain the vitrification time. The first one is based on the criteria of maximum tan δ peak at 1 Hz, and secondly, the criteria based on maximum G″ peak at 1 Hz. Fig. 3(d) depicts vitrification times from rheology measurements at 120 °C based on the selected criteria. An enhanced value for vitrification is always noted based on the latter criterion.

3.3. Mechanical properties and modification

In the cure polymerization reaction, the main steps are conversion and formation of cross-links to form a thermoset polymer. Chain extension of the system may be made possible by the chemical reaction between the hydroxyl end of HTPB and hardener and also by the ring opening reaction [10]. This may lead to an increase in toughness of the epoxy network. The toughness enhancement is also due to the increase in degree of entanglement between the resin and the rubber [34]. Increase in main chain mobility also favors the property improvement [35].

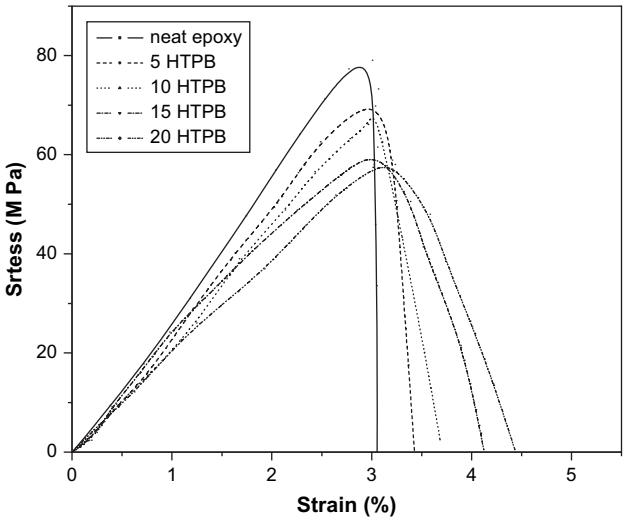

Fig. 4. Stress versus strain curve.

3.4. Tensile strength and related properties

Stress–strain behaviors of the modified epoxies are shown in Fig. 4. The neat resin system exhibits a brittle tensile behavior characterized by a Young's modulus value of 1913 MPa. Addition of HTPB decreases Young's modulus showing ductile nature of modified systems. Generally, when a rubber modifier is added to a thermoset resin, its elastomeric character authorizes a decrease in Young's modulus, significantly. This was noted when a CTBN modifier, which was initially partially miscible with the resin, was employed during the toughening study of epoxy resin by the authors [36]. The Young's modulus changes to a value of 1457 MPa, as compared to the above reported value of the neat epoxy, upon the addition of 5 wt% of CTBN. Whereas, in the present case, the modification by 5 phr HTPB permits a change in the value to only 1814 MPa. The system became more ductile upon CTBN addition. The very slight reduction in the values of HTPB-modified epoxies may be attributed to the lowering in cross-linking density of the epoxy network as the modifier occupies the reaction centers during modification. The various tensile properties for different loadings of the rubber are formulated in Table 3. The decrease in tensile strength with

Table 3
Tensile properties at room temperature with different loadings of rubber cured at 180 °C

HTPB (phr)	Tensile strength (MPa)	Young's modulus (MPa)	Modulus at 2% elongation
0	79	1913	1850
5	73	1814	1766
10	66	1765	1746
15	61	1706	1697
20	58	1667	1648

rubber content can be related to stiffness of the modified network. The rubber addition decreases stiffness of the network epoxy probably due to lowering in cross-linking density. Since HTPB is less compatible with the resin, the volume fraction of the dispersed rubber phase becomes more significant that reduces the interaction in the epoxy matrix. The volume fraction of rubber increases with the increase in the addition of the elastomer.

3.5. Fracture properties

Pre-reaction of the rubber with the hardener imparts interaction between rubber particles and epoxy matrix during curing. Change in the values of fracture toughness (critical stress intensity factor, K_{1C}) and fracture energy, (critical strain energy release rate, G_{1C}) as a function of rubber weight percentage are furnished in Fig. 5. The generally reported value of K_{1C} for most of the neat epoxy resin [5] is below 1.5 M $Nm^{3/2}$. The addition of rubber imparts an increase in the value of K_{1C} up to an optimum rubber content of 10 phr. Fracture energy also shows the same trend. No further increase was found on further loading of rubber. This may be attributed to the bigger size of rubber particles at higher concentrations. As noted from SEM pictures there is an increase in the size of particles for 15 and 20 phr HTPB blends. Further there is a change to multi-modal size distribution of particles. The large particles obtained at high rubber content would deteriorate impact toughness as this would result in high stress intensities around the agglomerated rubber particles.

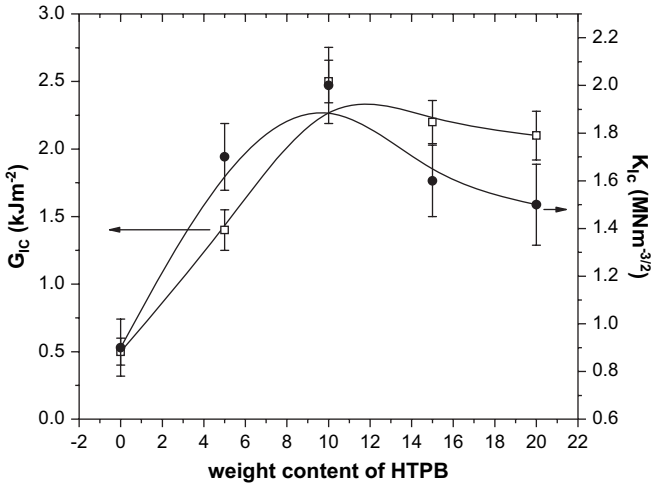

Fig. 5. Fracture toughness and fracture energy as a function of rubber content.

The improvement in toughness, as explained by Kinloch and Hunston [37], is attributed due to rubber particles that enhance shear localization by acting as stress concentrators. Hydrostatic tension ahead of the crack tip causes rapid cavitations of the rubber. The voided damage zone then blunts the crack, which behaves as if it had a much larger crack tip radius. Thus a larger plastic zone gets associated with this crack and this is the source of toughening effect. The rubber particles that are bonded to the matrix can bear the load in triaxial tension. Thus interfacial interactions of rubber particles with the matrix epoxy is desirable for toughness property which can be attributed by pre-reaction of the rubber thereby improving toughness by increasing the miscibility of rubber into the epoxy matrix. Hence some amount of rubber goes into the epoxy matrix and act as plasticizer. If rubber is incorporated into the epoxy network, it acts as a flexibilizer. Both of these effects increase the ability of the matrix to deform under shear. But, since HTPB has no appreciable miscibility with the resin, plasticization of the matrix is practically zero, and only flexibilizing effect operates. This is, perhaps, the reason for the slow increase of K_{1C} values with rubber loading. The curing followed by the phase separation of the elastomer phase is schematically represented in Fig. 6. Fig. 6(A) represents individual

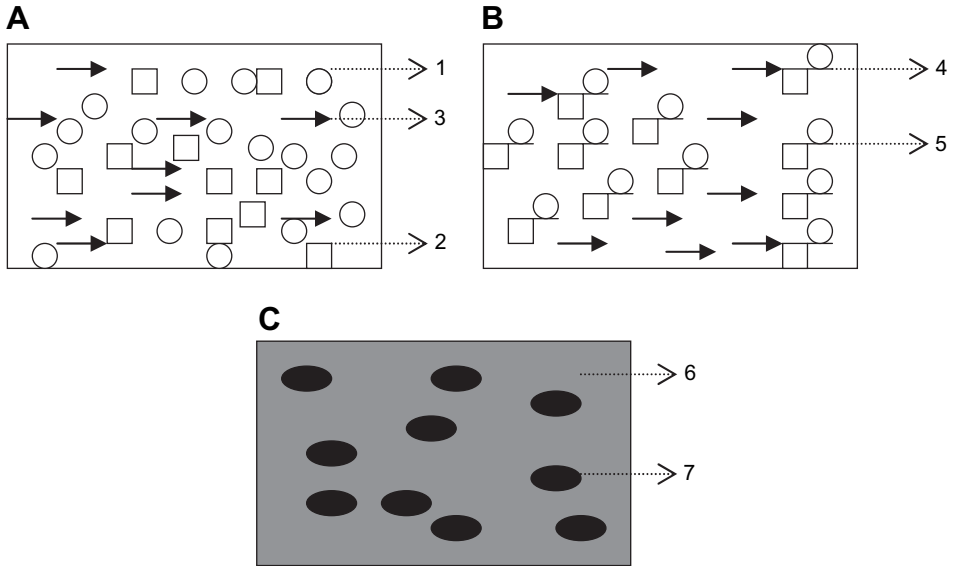

Fig. 6. Schematic representation of phase separation behavior. 1, 2, and 3 represent individual epoxy, hardener and elastomer units; 4 and 5 symbolize, respectively, the bonding of elastomer–hardener–epoxy and hardener–epoxy; 6 and 7 correspond to three-dimensional base matrix of epoxy network and domains of phase separated neat HTPB.

components present in the system: the circle, the square, and the arrow represent epoxy, hardener, and rubber units, respectively. The polymerization starts mainly with the reaction between hardener and epoxy, represented by the bond formation between them. During the cure reaction few of the elastomers react with the hardener, forming elastomer–hardener–epoxy network. Most of the HTPB units remain as such without involving in the cure reaction. Part figure (B) represents this state of curing. Meanwhile, as the molecular weight of the system increases, rubber gets phase separated to form domains, which are almost pure HTPB. This is depicted by the representation (C) in the figure.

Also, the SEM micrographic studies of the fractured surfaces of samples show stress-whitened zone near the crack tip, which is supposed to occur by micro-cavitations of rubber particles due to high hydrostatic stress beneath the blend crack tip. The SEM photograph of a 10 phr rubber-modified epoxy (Fig. 7) clearly demonstrates this. Detailed microscopic examination of the stress-whitening region proved presence of small closely spaced holes. The presence of such holes is interpreted as caused by the dilatational deformation of the particles and the matrix [38,39] that nucleates local shear yielding of the epoxy matrix causing a significant crack tip deformation. The crack growth resistance of rubber-modified epoxies arises from the energy dissipation occurring in the vicinity of crack tip. The synergic effects of localized cavitations at the rubber/matrix interface and plastic shear yielding in the epoxy matrix are supposed to be responsible for deformation that results in energy dissipation process which ultimately improves the fracture toughness values of the rubber-modified epoxies.

3.6. Impact property

The results of impact strength of neat epoxy and resin samples containing different amounts of the rubber are depicted in Fig. 8(a). All modified networks show higher impact resistance than neat resin. However, the property attains a maximum for 10 phr rubber content and above this optimum level of rubber content a falling tendency was noted. The increase in value upto an optimum level of rubber concentration is attributed to the effective stress concentration behavior of the phase separated rubber-rich particles that amplify plastic deformation of a highly brittle matrix to a certain extent. The blend network containing a 10 phr rubber has a maximum impact strength value of 13.6 J/m^2 which is about 47% higher than that of neat epoxy and for a 20 phr rubber the value is 30% lower than the maximum. However, 20 wt% blend exhibits a better performance than the neat one. In a work done by Ratna [40], using carboxyl terminated poly(2-ethyl hexyl acrylate) rubber (CTPEHA) to modify an epoxy matrix, a 60% improvement in impact property was reported. Comparatively lower performance of the present rubber shall be attributed to lesser compatibility with the epoxy resin. The decreasing tendency of impact strength after an optimum level of 10 phr rubber inclusion is attributed to the aggregated size of rubber particles as concentration of rubber increases. Similar behavior has been also reported in other rubber-modified epoxy systems [7,41]. Large elastomeric domains act as deflection sites and lead to catastrophic failure of matrix. However, matrix ductility attained by the incorporation of rubber is responsible for the improvement of impact strength of the higher modified blend in comparison to that of neat epoxy. The influence of matrix ductility on impact strength behavior has been well explained in certain rubber-modified epoxy systems [42,43]. The improvement in impact strength shall be correlated with toughness enhancement. The impact strength measurement is very sensitive to imperfections of the specimens. Imperfections due to voids, bubbles, and inclusions may affect the results of impact strength. For an unnotched specimen, stress may not concentrate on a specific point and the material undergoes fracture at the weakest point. Thus normally impact strength of samples may not be complementary to that of tensile test results.

With a view to investigate the relation between cure temperature and impact strength, a modified sample containing 10 wt% HTPB has been investigated. As shown in Fig. 8(b), the impact strength of modified epoxy networks increases slowly and attains a maximum at 160 °C. A comparatively lower value is noted for a high temperature cured sample. The morphology of samples at a high T_{cure} was found to be noticeably different from that of a low temperature cured one and this difference in morphology shall be a parameter which influences the impact nature. The morphology of the modified epoxies cured at 160 and 200 °C are portrayed in Fig. 8(c) (i) and (ii), respectively. Well-defined domain distribution of particles is clearly observable in the SEM photograph of the blend cured at 160 °C, which was found to be the optimum cure temperature. Whereas in the blend of the same composition, but $T_{cure} = 200$ °C, domain distribution is not uniformly defined. This shall be attributed to the fact that phase separation started well before gelation, and since high temperature leads to fast curing, particle growth was not effective due to restriction caused by diffusion in the epoxy matrix. Well-distributed particles in the matrix can build up better energy dissipation, which leads to significant impact behavior of the matrix. Similar results are reported in the case of elastomer-modified epoxies [44] and thermoplastic toughened epoxies [45].

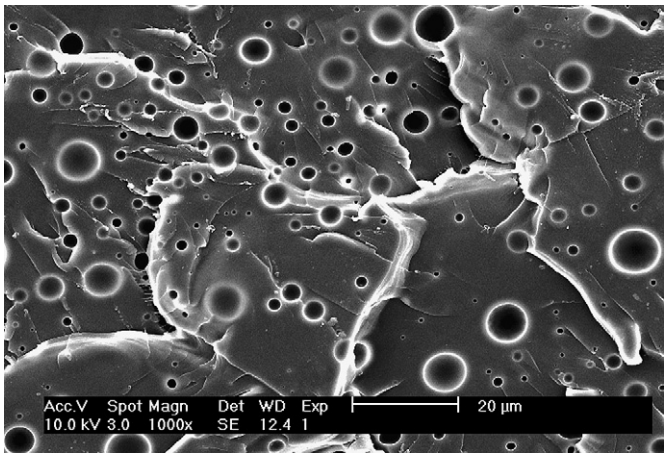

Fig. 7. SEM micrograph of 10 phr HTPB blends showing stress-whitened zone.

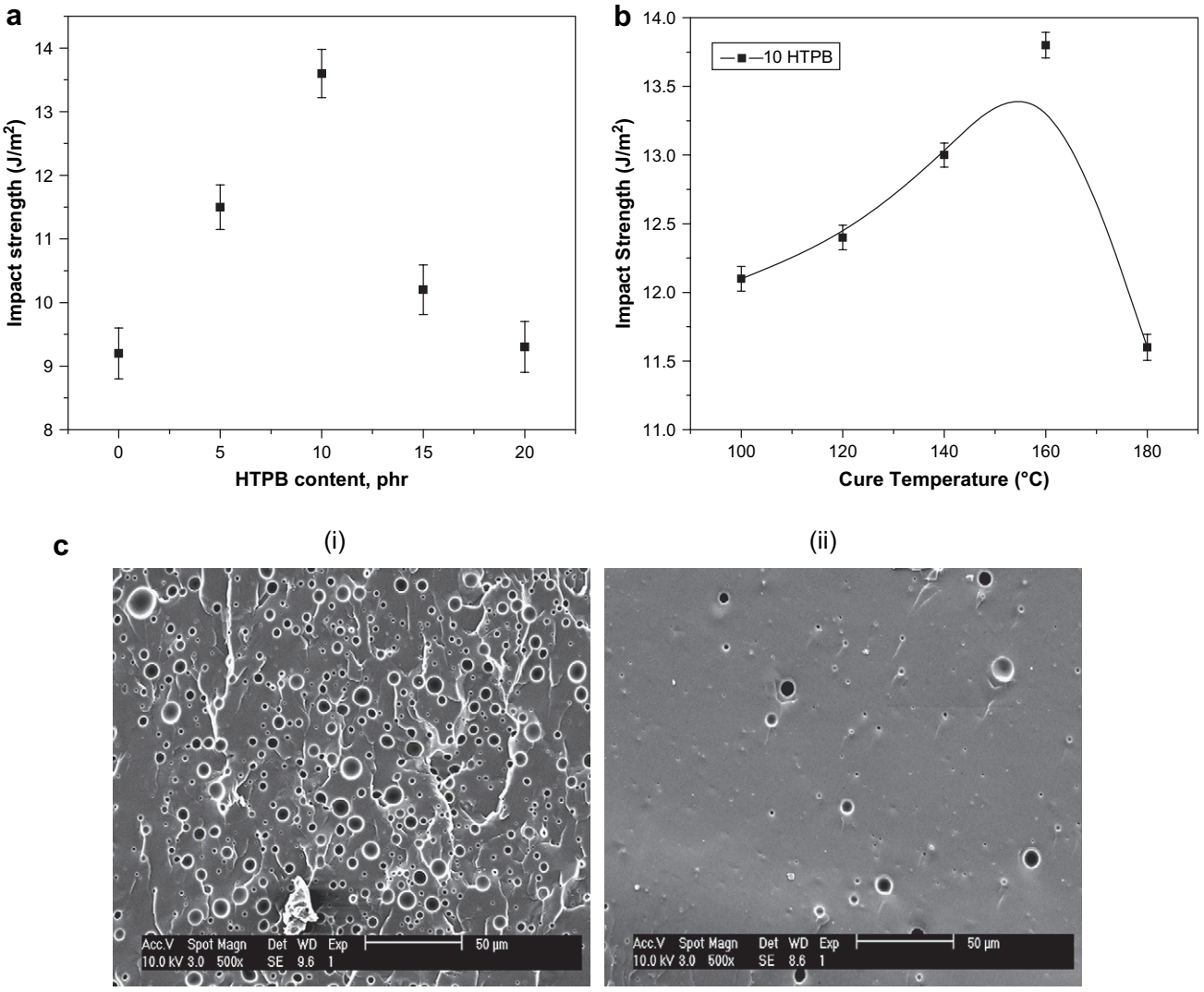

Fig. 8. (a) Impact strength of neat and cured blends. (b) Impact strength of 10 phr rubber blend cured at different temperatures. (c) (i) and (ii) SEM micrographs of modified epoxies cured at 160 and 200 °C.

It is important to add that the high temperature cured sample may not get sufficient time to develop particle growth effectively and hence shows almost single phase morphology on the fracture surface which results in poor impact performance. However, they show high impact performance compared to neat epoxy samples. This is due to the phase separated nature in these samples, even though not well-defined, unlike in the unmodified one. It is widely accepted that phase separation is a necessary criterion for toughening in rubber-modified epoxies. Therefore compared to the neat epoxy matrix the high temperature cured network shows a higher toughness and impact strength. The ductility of the modified matrix imparts absorption of energy, which ultimately leads to toughness characteristics [46].

3.7. Flexural properties

Fig. 9 depicts the flexural properties of neat and rubber-modified resin samples. The flexural strength and modulus

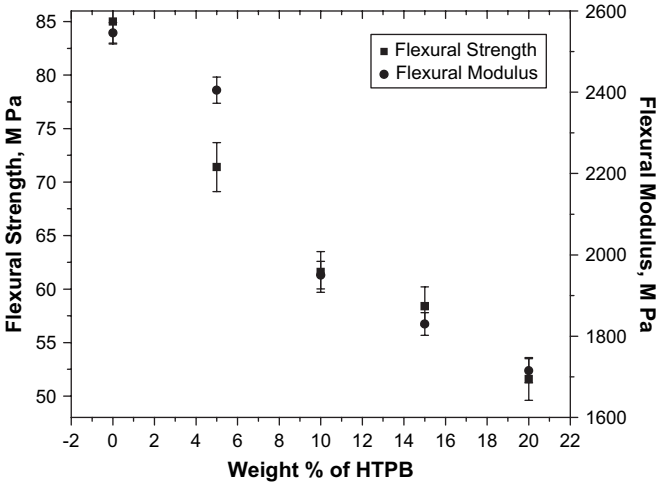

Fig. 9. Flexural properties of neat and modified epoxies.

of the modified samples are lower than that of the unmodified epoxy. The phase separated low modulus rubber domains impart reduction in modulus. A very small amount of rubber may get incorporated into the epoxy matrix, thereby flexibilizes the thermoset network. The rubber that is incorporated into the resin matrix is responsible for the reduction in flexural strength of the modified samples. Previous works on rubber-modified epoxies support this observation [8,9,34,47,48].

3.8. Morphology and toughening behavior

The fractured surfaces of the specimens were examined using scanning electron microscopy (SEM). Typical fracture surfaces of neat and that of modified epoxies are shown in Fig. 10. The neat epoxy matrix, Fig. 10(a), shows smooth, glassy, and rivery fractured surfaces with ripples. The relative smoothness of the fractured surface, irrespective of the presence of some shear deformation lines, indicates that no significant plastic deformation had occurred. The morphological development during cure can be correlated with the impact behavior. The ripples are due to the brittle fracture of the network, which accounts for its poor impact strength, as there is no energy dissipation mechanism operating here.

But the cryogenically fractured surface of the modified epoxies, Fig. 10(b)–(e) (representing 5–20 phr rubber-modified epoxies), clearly show two distinct phases – a continuous epoxy matrix and the dispersed rubber phase. This heterogeneous morphology resulted opacity in samples. The holes developed in the SEM micrographs are due to the extracted particles from the surface of the samples after treatment with toluene for 12 h. The domain parameters of the phase separated elastomer are measured and are furnished in Table 4. The size of the precipitated rubbery domains increases with increase in elastomer content of the formulations. Number and area average domain diameters are found to increase with respect to rubber content, which is in agreement with the behavior of other rubber-modified epoxies. The inter-particle distance of the rubber domains is also estimated and found to increase with higher inclusion of

Table 4
Number, area, weight, and volume average diameter of domains dispersed in the epoxy matrix

HTPB content (phr)	D_n^a	D_a^b	D_w^c	D_v^d	D_w/D_n	Inter-particle distance (μm)
5	0.82	0.85	0.91	1.46	1.10	0.91
10	0.90	0.96	1.07	1.52	1.18	1.23
15	1.2	1.4	1.7	2.3	1.41	1.42
20	1.5	1.8	2.2	2.8	1.52	1.64

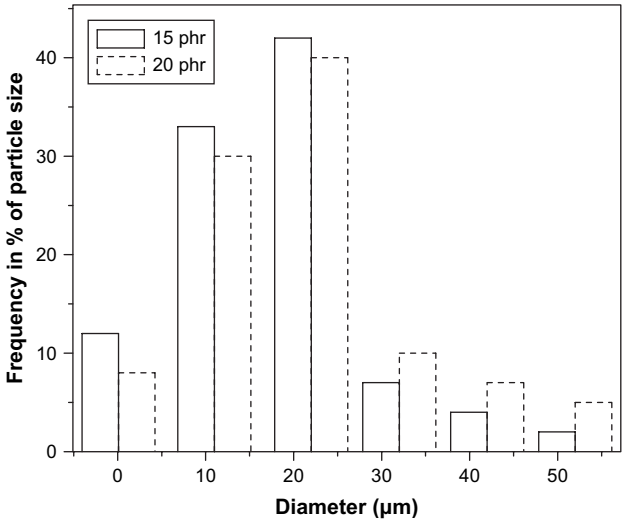

Fig. 11. Particle size distribution in 15 and 20 phr rubber–epoxy blend.

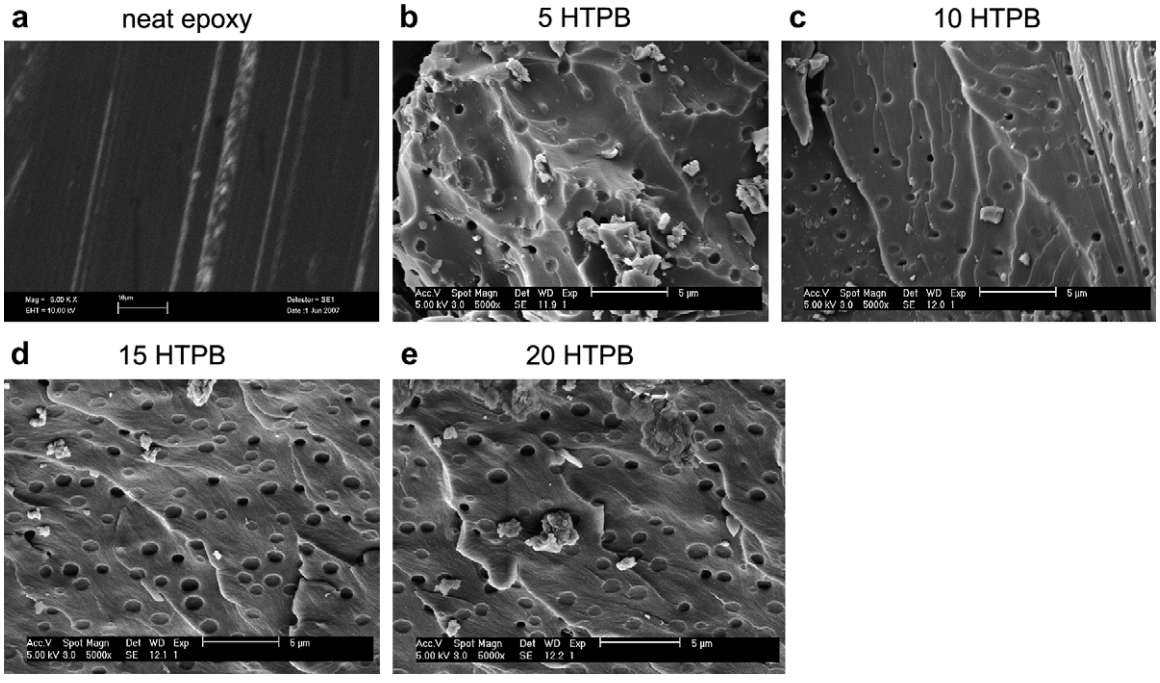

Fig. 10. SEM micrographs of: (a) neat epoxy, (b) 5 phr blend, (c) 10 phr blend, (d) 15 phr blend and (e) 20 phr blend.

rubber demonstrating lesser interaction of rubber with the epoxy matrix. The increase in domain size with the incorporation of rubber is attributed to the coalescence of the dispersed rubber particles, which depends on viscosity and elasticity ratio. This becomes more prominent in higher weight content of the dispersed rubber phase. In epoxies with 5 and 10 wt% of rubber, as shown in Fig. 10(b) and (c), the particles are uniformly distributed throughout the matrix with a narrow particle size distribution. This unimodal distribution of smaller particles is responsible for lower crack growth in these specimens which is indicated by the presence of relatively large number of deformation lines. Also, the fracture surfaces, unlike neat epoxy, are not very smooth, indicative of a ductile manner of fracture. According to Yee and Pearson [49], the size of stress-whitened zone or the amount of deformation lines is proportional to the increase in toughness of the material. Relatively distorted shape of rubber domains in these cured resin matrices is supposed to be attributed to higher amount of plastic deformation. The deformation lines are propagated through rubber domains, promoting stress transfer between the

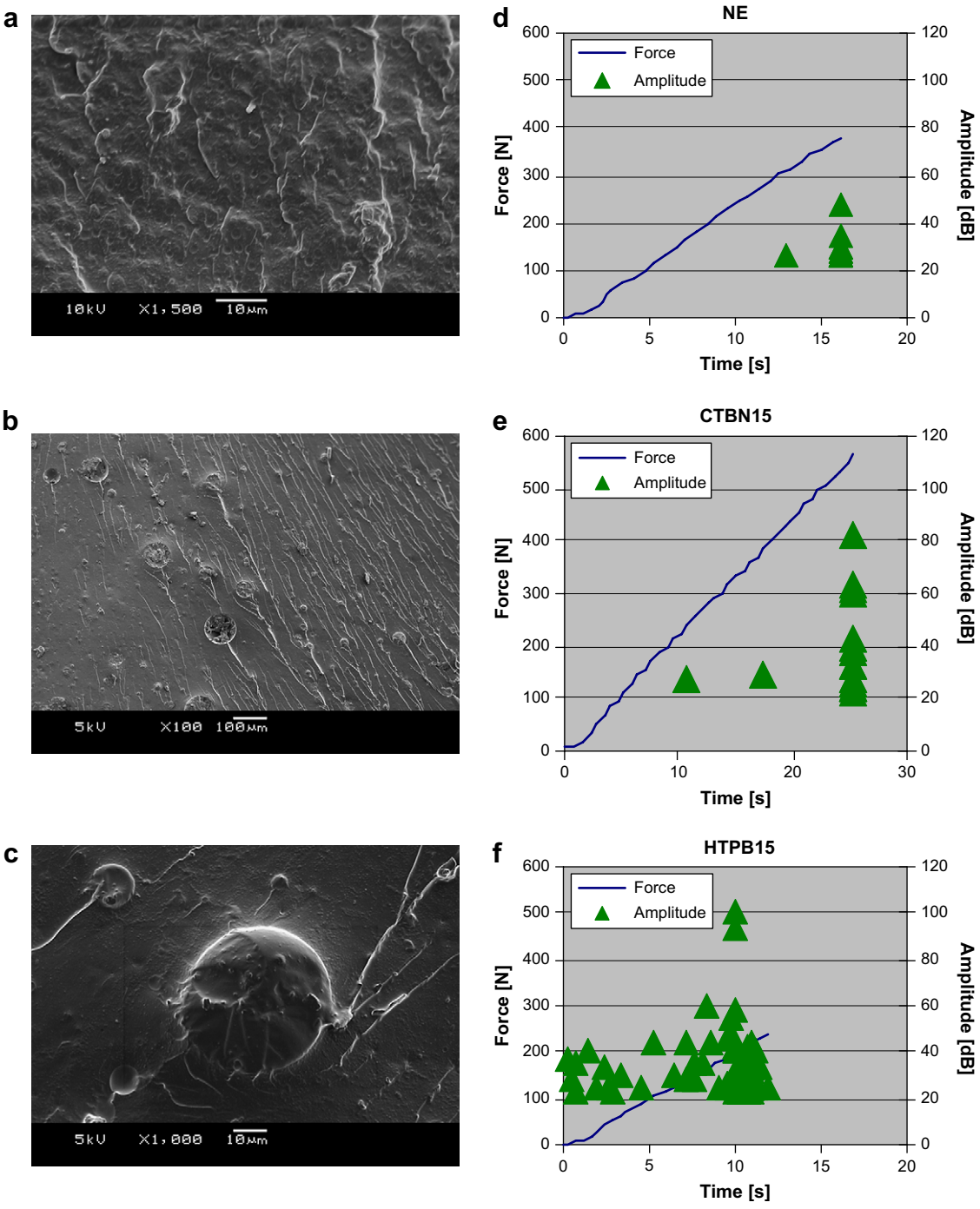

Fig. 12. (a) SEM micrographs of 15 phr HTPB–epoxy blend. (b) SEM micrographs of 15 phr CTBN–epoxy blend. (c) HTPB aggregation in 15 wt% blend. (d) Amplitude signal of neat epoxy. (e) Amplitude signal of 15 phr CTBN blend. (f) Amplitude signal of 15 phr HTPB blend.

particles and epoxy matrix. Also, less brightness of the interfacial layer around the rubber domains in lower modified epoxies compared to higher modified samples is indicative of the interaction between the particles and epoxy matrix [10]. The micrographs show stress-whitened zone of broken rubber particles. According to Lee et al. [50] and Bascom and Hunston [51], the stress-whitening is due to the scattering of visible light from the layers of the scattering center which are voids developed in the matrix due to cavitations of rubber particles. This has been explained by researchers as one of the most important energy dissipation mechanisms operating in rubber-modified epoxies.

In order to operate the yielding process throughout the matrix, a homogenous distribution of smaller particles is necessary. This morphological structure is believed to be responsible for the highest impact performance of modified epoxies. Thus uniformly distributed rubber particles act as stress concentrators and exhibit highest impact strength than unmodified epoxy.

In higher weight percentage of rubber-modified samples, say 15 and 20 phr which are represented by (d) and (e) of Fig. 10, a heterogeneous particle size distribution is observed. The particle size distribution in a blend containing 15 and 20 phr rubber is illustrated in Fig. 11. The particle size distribution has a wide range from 0.1 to 75 μm. Most of the particles are situated in the range of 15–28 μm. The frequency of percentage of higher particle size is predominant in modified epoxies containing higher weight content of the elastomer. The heterogeneous morphology developed in high concentrated blends can be correlated with gelation time. The gelation time increases as the concentration of the rubber increases due to viscosity and reduced reactivity factors. The number of particles having bigger sizes increases with the inclusion of higher concentration of elastomer. This results in wide variation of size distribution. The poor mechanical performance of higher modified systems shall be attributed also to this heterogeneous nature of particle size distribution.

In an attempt to recognize the failure mechanism in HTPB-modified epoxies we have analyzed the samples with the help of acoustic emission method during static tensile test of single-edge notched specimens (SEN-T specimens). It is a non-destructive and very sensitive technique to monitor the fracture of composites. For a comparison, the results of conventional CTBN elastomer-modified epoxies are also recorded. Different failure mechanisms were assigned to different signal levels determined on the basis of the number of acoustic events. The acoustic hits detected for neat and 5 phr HTPB/CTBN-modified epoxies are 20 ± 6, 38 ± 4 and 37 ± 5, respectively. The increase in acoustic events for toughened epoxies clearly shows homogeneous distribution of elastomer in the epoxy matrix. When the material undergoes fracture, crack is propagated through elastomeric domains via an energy dissipation mechanism and this is due to the damping nature of the toughened epoxy. Further it is to be noticed that for 15 wt% HTPB/CTBN-modified epoxies acoustic events changed to a value of 101 ± 10 and 27 ± 5. One will definitely notice the almost similar value of CTBN-modified specimens and the incomparable values of HTPB blends with the values of lower modified epoxies. The drastic change in the value of HTPB–epoxy blend is attributed to the magnifying change in the morphological evolution of the blend at higher concentration of the elastomer. Two representative SEM micrographs of 15 phr HTPB/CTBN blends are depicted in Fig. 12(a) and (b). Heterogeneity is observed in the size distribution of HTPB–epoxy blend, whereas, a homogenous distribution of particles is observed in CTBN sample. Fig. 12(c) represents formation of bigger particles in 15 wt% HTPB elastomer-modified blend. The amplitude of signals detected during fracture varies widely for these systems. The signals measured during the fracture of neat epoxy (NE) are in the region of 20–50 dB whereas it goes upto 100–120 dB for CTBN filled epoxy. But for HTPB-modified epoxy signals are observed in the range of 21–42 dB and are detected throughout the whole measurement. The high amplitude signals at the end of the measurement, for all systems, represent epoxy break. The force response and amplitude of signals for neat and both CTBN/HTPB-modified systems (15 wt%) are represented in Fig. 12(d)–(f). The signals observed for a 15 phr HTPB sample throughout the measurement denotes the pull-out and breakage of rubber particles in the sample containing higher weight percentage elastomer. The deterioration in fracture and damping properties of higher weight percentage of HTPB-modified epoxies is clearly due to this. However, for CTBN sample the signals are observed only at the end of the measurement. Knowing the fact that the lower elastomer incorporation enhances fracture properties whereas the inclusion of higher weight percentage of elastomer content

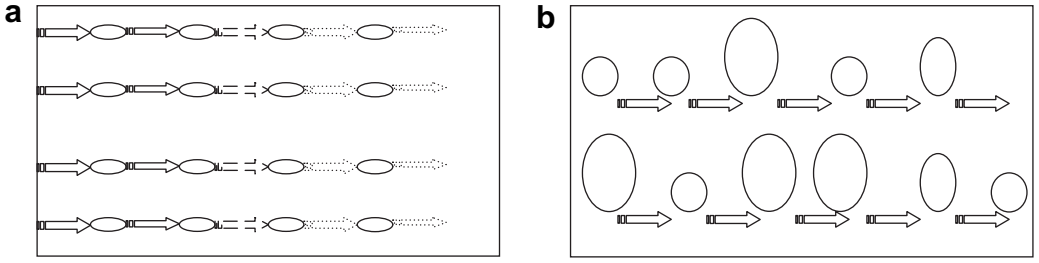

Scheme 2. Schematic representation of toughening mechanism in epoxy–HTPB blends. (a) Represents lower weight percentage of HTPB-modified epoxy. The arrows denote the crack energy propagation through rubber particles. The intensity of energy decreases as it passes through rubber particles. (b) Represents higher weight percentage of HTPB-modified epoxy. Elastomer domains are pulled-out from the matrix. The crack energy propagates through the interface of rubber and epoxy. There is no decrease in the propagated intensity of energy.

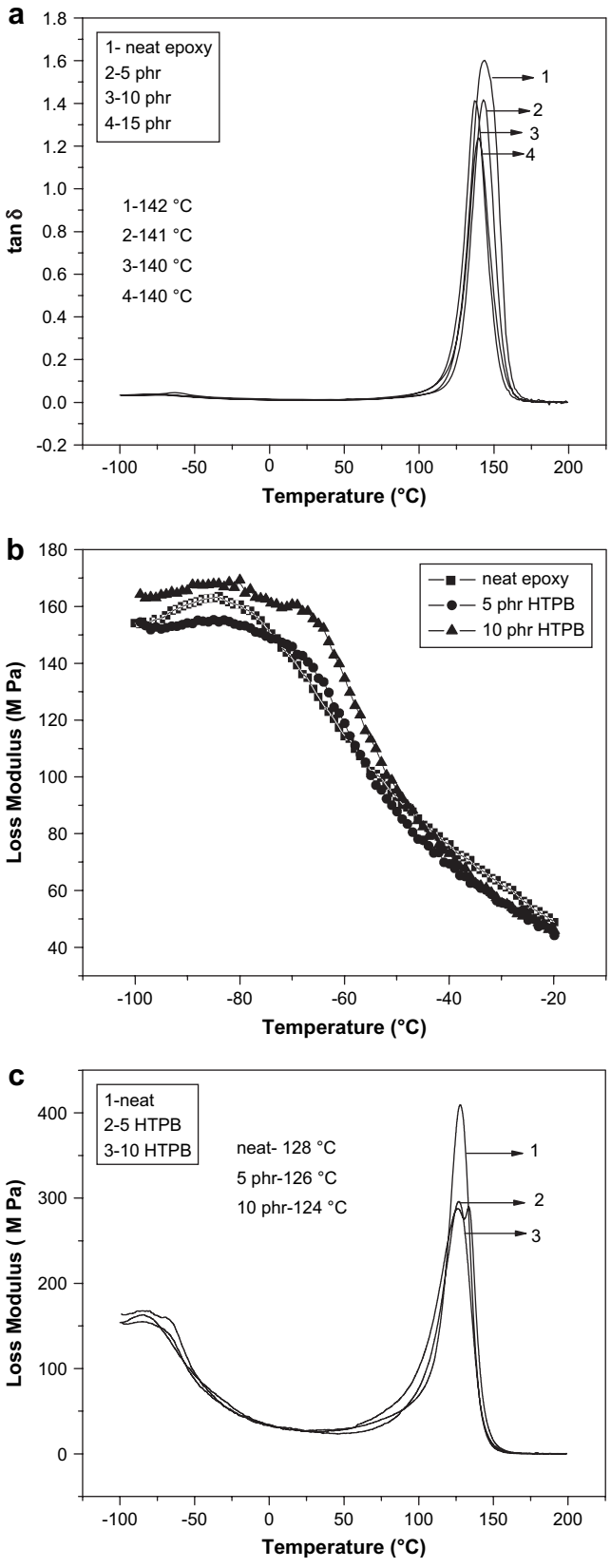

Fig. 13. (a) Dynamic loss factor, tan δ versus temperature of the neat and modified epoxies. (b) Low temperature region of the curves in Fig. 13(a). (c) Loss modulus curves of pure and modified blends.

deteriorate them, and also from the acoustic emission results, we would like to propose an ''elastomer pull-out'' model of failure mechanism operating in HTPB toughened epoxies. The homogeneous distribution of elastomer particles in lower modified epoxies is responsible for the enhanced damping nature of the samples. The particles in such systems act as stress concentrators and during failure, on applying force, energy transfer take place through particles and dissipate in due course. Thus ultimately the matrix is protected from catastrophic failure. This state is schematically represented in Scheme 2(a). The spherical shapes denote elastomeric particles adhered to the matrix epoxy. The arrow represents the crack energy propagation from the crack initiation site, which gradually reduces as it passes through elastomeric particles. The dissipation of energy is represented by the reduction in the size and diffusivity of the solid line nature of the arrow. The dotted line arrow shows that the initial energy reduces as it passes through rubber particles. The particles get distorted as it propagates energy, but this is not represented in the scheme. Scheme 2(b) represents higher weight percentage rubber-modified epoxies characterized by elastomeric particles having larger sizes and having less interfacial adhesion. The orientation of particles in the upward direction represents pulling-out of the particles. Arrows represent the crack propagation through the interface. There is no reduction in the crack energy intensity as it is not propagated through elastomers, which is denoted by the same style of arrows. This creates interfacial separation which ultimately leads to failure of the matrix.

3.9. Dynamic mechanical properties (DMA)

Dynamic mechanical loss factor (tan δ) versus temperature of pure epoxy resin (ER), and representative modified networks of 10 and 15 wt% of HTPB are depicted in the Fig. 13(a). The neat epoxy resin shows a peak at around 142 °C, which is clearly related to the glass transition temperature of the ER. The presence of HTPB results only in a slight displacement of the transition peak; for e.g., for 5 and 10 phr modified epoxy networks a shift to a lower region is observed by a shift of 1 and 2 °C, respectively. This may be attributed to the lowering of cross-linking density in the modified samples. During the curing of epoxy resin, phase separated rubber domains shall occupy the space in between the reaction sites, thereby impairing the cross-linking reaction at that particular site. This, in turn, reduces the cross-linking density of cured systems. Thus the overall cross-linking density changes by the incorporation of more rubber.

The low temperature transition peaks are presented in Fig. 13(b). The virgin epoxy shows a transition near −80 °C, which is associated with the epoxy resin β-relaxation. However, it seems difficult to differentiate this transformation from that of the relaxation allied to the rubber phase, as both of these transitions appear almost in the same region. Rubber-modified networks also show slight displacement of this transition towards the higher temperature region. Thus, this technique, in the present case, seems inadequate to distinguish

the relaxations related to the elastomer phase. This observation contradicts with other rubber-modified epoxies. Thus in the case of CTBN-modified epoxies, as reported elsewhere [18], the low temperature transitions of the modified networks are significantly shifted to higher temperature, showing that the phase separated rubber domains are not pure, instead, contain some dissolved epoxy. Thus having considering the fact that the modified network does not show significantly noticeable displacement of relaxation in high and low temperature region and also by morphological observation by SEM, one presumes that the phase separated elastomer particles are pure and does not contain dissolved epoxy. The variation of the ultimate morphological evolution in cured systems with different weight percentage of rubber arises from the dissimilarity in cross-linking density and size of rubber domains. Fig. 14(A) and (B) schematically demonstrates this difference in the final morphology in cured systems. Network lines symbolize cross-linking state whereas spherical shapes represent elastomer domains. The part figure (A) represents the morphological evolution when a lower weight content of rubber is employed. The morphology is characterized by more cross-linking behavior and inclusions of small rubber domains. On the other hand, the part figure (B) shows the difference by the presence of comparatively bigger rubber domains and fewer cross-linking nature, the one addressed to a modified epoxy with higher weight content of rubber.

Fig. 13(c) represents the DMTA data for pure epoxy and 5 and 10 phr rubber-modified epoxy. The modified networks show two relaxation peaks: one at ca. 128 °C for epoxy and the other at ca. −82 °C which can be assigned to the glass transition of rubber. The pure epoxy also shows a broad peak at low temperature region as in the tan δ relaxation curve, which is often attributed to crankshaft motion of the glyceryl-like groups in DGEBA [52,53]. The slight shift in relaxations towards lower temperature region in modified epoxies is attributed to lowering in cross-linking density.

The cross-linking densities of epoxy–rubber blends have been computed using the expressions (5) and (6). The values are in the order of 10^{24} and were observed to be 1.75, 1.73, 1.71, 1.69 and 1.68 chains/g, respectively, for neat resin, 5, 10, 15 and 20 phr HTPB. The molecular weight between cross-links increased with the addition of elastomer to the epoxy resin and consequently cross-linking density decreases. Also, the gradual drop of storage modulus with the addition of the elastomer denotes the increase in flexibility of blend samples. The drop in storage modulus with increasing temperature indicates that all modified epoxies passes from hard solid to soft flexible materials. The storage modulus of the modified epoxies in the rubbery plateau region, $T_g + 50$ °C, shows a decreasing trend from neat epoxy indicating the reduction in cross-linking density. The value decreases from 5% for 5 phr to 10% for 20 phr elastomer content.

3.10. Thermogravimetric study

Thermal stability and thermal degradation behavior of the modified samples are derived from TGA traces. Fig. 15(a) and (b) shows TGA and DTA thermograms of the neat and 10 wt% modified samples obtained in a nitrogen atmosphere. The anhydride-cured epoxy samples undergo the degradation mainly as a two-stage process. The neat and modified systems exhibit a short stage of degradation around 250 and 225 °C with an approximately 5% weight loss. This is attributed to the breaking of unreacted epoxy or other traces of impurities apart from the cured resin. The main degradation takes place above 565 °C and is due to the thermal degradation of the epoxy network [54]. The degradation temperature and kinetic parameters of the reaction, such as initial decomposition temperature (IDT), temperature of the maximum rate of degradation (T_{max}), and the activation energy of decomposition (E_1) can be used to ascertain a materials lifetime [55,56]. The values of IDT and T_{max} for neat and 10 phr rubber-modified cured sample are furnished in Table 5. A higher value of IDT for the neat system can probably be attributed to the higher cross-linking density of the system. Inclusion of HTPB creates domains of rubber particles in between the cross-links which ultimately reduce the cross-linking density.

Using the integral method of Horowitz and Metzger [57], one calculates the activation energy for the decomposition of the cured resin from TGA thermograms according to the following equation:

$$\ln\left[\ln(1-\alpha)^{-1}\right] = \frac{E_1\theta}{RT_{max}^2} \tag{7}$$

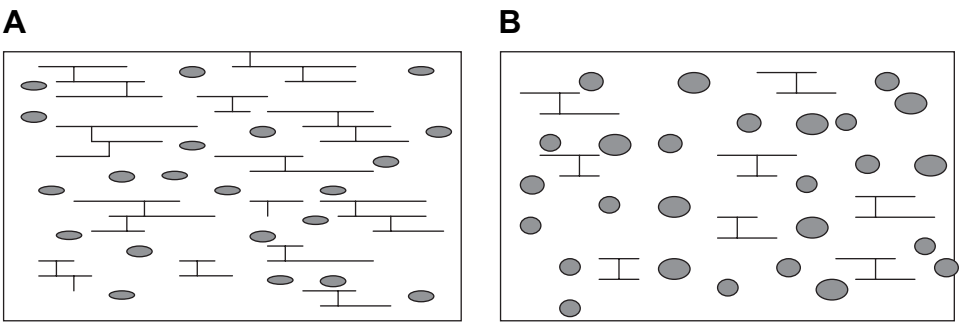

Fig. 14. Schematic presentation of morphological evolution at different cure temperatures. Cross-linked lines and darkened circles represent epoxy network structure and phase separated rubber domains, respectively. Scheme A defines higher cross-linking nature and small rubber particles on the inclusion of lower weight percentage of rubber whereas scheme B is distinguished by fewer cross-linking lines and comparatively larger elastomer domains on the incorporation of a higher content of rubber.

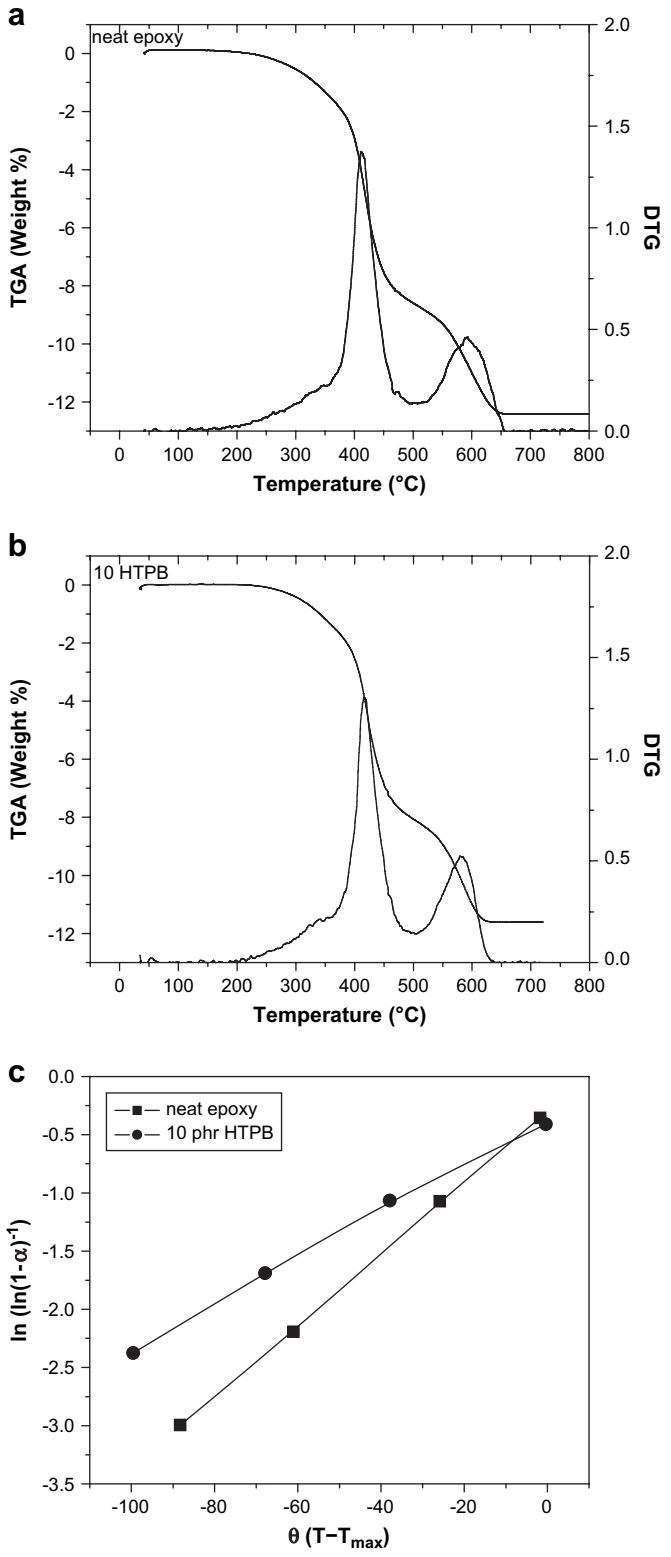

Fig. 15. (a) TGA thermograms of neat epoxy. (b) TGA thermograms of 10 phr rubber–epoxy blend. (c) Plots of $\ln[\ln(1-\alpha)^{-1}]$ versus θ for neat and 10 wt% rubber blend.

where $\alpha =$ decomposed fraction; $T_{max} =$ temperature at the maximum rate of weight loss; $\theta = T - T_{max}$; $R =$ gas constant.

The plots of $\ln[\ln(1-\alpha)^{-1}]$ versus θ are shown in Fig. 15(c) where the slope of the straight line curves gives E_1 values of the systems and are tabulated in Table 5. The E_1 values of the neat and 10 wt% modified systems are 105 and 95 kJ/mol, respectively. The result, once again, emphasizes the higher cross-linking density of the neat system, which needs more activation energy for degradation.

Table 5
Thermal properties of cured neat and modified epoxies

Epoxy system	IDT (°C)	T_{max} (°C)	E_1 (kJ/mol)
Neat epoxy	300	565	115
Epoxy + 10 phr HTPB	282	560	95

3.11. Concluding remarks

Functionally terminated polybutadiene liquid rubber has been incorporated into the epoxy resin matrix that undergoes curing with an anhydride hardener. Inclusions of rubber, as observed from DSC analysis and gel point determination, caused delay in polymerization and hence delay in gel time. This shall be attributed to the reduction in concentration of reacting species and viscosity effect on the addition of rubber. This was, further, confirmed by rheological analysis where an increase in viscosity was observed as a result of modification. Addition of rubber causes lowering in cross-linking density of epoxy matrix during the cure polymerization reaction. The mechanical performance of neat epoxy was changed with the inclusion of varying weight percentage of HTPB, which was explained by the evolution of morphological changes during cure in these systems. The elastomeric nature of the rubber caused reduction in tensile strength, but fracture toughness values increased and attained a maximum for 10 phr rubber inclusion. Some amount of added rubber goes into the epoxy matrix and flexibilizes the brittle thermoset matrix. This effect is responsible for the deformation under shear of the matrix, and thus for the prevailing toughening effect. Maximum impact property was observed for 10 phr rubber–epoxy blend attributed to the presence of uniformly distributed rubber particles. Further, impact strength was observed to be higher as cure temperature decreases. This is due to the lesser extent of particle growth attributed to fast curing of epoxy matrix at high temperature. The flexural properties were found to decrease by the inclusion of rubber. The fractured surfaces of modified epoxies were subjected to quantitative analysis to estimate various parameters of phase separated domains. The size of elastomer domains increased with the inclusion of greater weight percentage of rubber. The poor performances of mechanical properties of modified epoxies containing more than 10 wt% of rubber are considered as due to larger particle size. Based on acoustic emission studies and morphology analysis, a model for the failure mechanism has been proposed. In modified epoxies having lower weight percentage of elastomer, crack energy is propagated through elastomer particles and ultimately leads to failure. But in higher weight percentage of elastomer-modified epoxies, elastomer pull-out directs the energy transfer through the interface which leads to interfacial separation and finally failure of the matrix.

The viscoelastic behavior of cured blends showed only minimal changes in the transition temperature towards the lower region from that of cured neat epoxy. The phase separated rubber domains decrease the cross-linking density of the network. A schematic model has been presented to symbolize the final morphology in cured samples. Finally thermogravimetric analysis has been employed to establish the thermal degradation behavior of modified samples. The TGA thermogram has been used to compute activation energy for the decomposition of neat and rubber incorporated blend samples.

Finally it is important that, even though HTPB has been presented as a modifier for toughening epoxy matrix in the literature, an in-depth understanding on different aspects of the system has not been documented. The present work tries to address and correlate many issues related to the modified epoxy so as to explain the structure–property relationship. Rheological transformations during curing, mechanical properties, viscoelastic behavior, morphological evolutions, activation energy based on thermogravimetric analysis all have been discussed and tried to correlate between them.

Acknowledgement

One of the authors (Mr. Raju Thomas) thanks the Katholieke University, Leuven, Belgium for analytical and financial support for the work. He also thanks Kerala Science, Technology, and Environment Department for an SRF project. The authors would like to thank Huntsmann for their kind supply of chemicals for the study.

References

[1] Lee H, Neville K. 'Epoxy resins' in EPST. 1st ed, vol. 6. The Epoxylite Corporation; 1967. p. 209–271. [Reprinted in 1982].
[2] Verchere D, Sautereau H, Pascault JP, Moschiar SM, Riccardi CC, Williams RJJ. J Appl Polym Sci 1990;41:467.
[3] Bartlet P, Pascault JP, Sautereau H. J Appl Polym Sci 1985;30:2955.
[4] Chen TK, Jan YH. Polym Eng Sci 1991;31:577.
[5] Bussi P, Ishida H. J Appl Polym Sci 1994;53:441.
[6] Bussi P, Ishida H. J Appl Polym Sci 1994;35:956.
[7] Latha PB, Adhinarayanan K, Ramaswamy R. Int J Adhes Adhes 1994;14:57.
[8] Barcia FL, Soares BG, Gorelova M, Cid JA. J Appl Polym Sci 1999;74:1424.
[9] Barcia FL, Amaral TP, Soares BG. Polymer 2003;44:5811.
[10] Ozturk A, Kaynak C, Tincer T. Eur Polym J 2001;37:2353.
[11] Boey FYC, Qiang W. J Appl Polym Sci 2000;41(6):2081.
[12] Boey FYC, Qiang W. J Appl Polym Sci 2000;76:1248.
[13] Muller R, Gerard E, Dugand P, Rempp, Gnanou Y. Macromolecules 1991;24:1321.
[14] Verchere D, Pascault JP, Sautereau H, Moschiar SM, Riccardi CC, Williams RJJ. J Appl Polym Sci 1991;42:701.
[15] Widmaier J. Macromolecules 1991;24:4209.
[16] Neilsen LE. J Macromol Sci Rev Macromol Chem 1969;C3:77.
[17] Bellenger V. J Polym Sci 1987;B25:1219.
[18] Thomas R, Durix S, Sinturel C, Omonov T, Goossens S, Groeninckx G, et al. Polymer 2007;48:1695.
[19] Jenninger W, Schawe JEK, Alig I. Polymer 2000;41:1577.
[20] Wise CW, Cook WD, Goodwin AA. Polymer 2000;41:4625.
[21] Flory PJ. Principles of polymer chemistry. Ithaca, NY: Universidad de Cornell; 1953.
[22] Su CC, Woo EM. Polymer 1995;36:2883.
[23] Martinez I, Martin MD, Eceiza A, Oyanguren P, Mondragon I. Polymer 2000;41:1027.
[24] Cracknell JG, Akay M. J Therm Anal 1993;40:565.
[25] Kim BS, Chiba T, Inoue T. Polymer 1993;34:2809.
[26] Harran D, Grenier-Loustalot MF, Monge P. Eur Polym J 1988;24:225.
[27] Flory PJ. Principles of polymer chemistry. NY: University of Cornell; 1988.
[28] Pillot C, Guillet J, Pascault JP. Die Angew Makromol Chem 1979;81:85.
[29] Yang IS, lee LJ. Polym Proc Eng 1987;5:327.
[30] Bakker CJ, St. John NA, George GA. Polymer 1993;34:716.
[31] Eloundou JP, Feve M, Harran D, Pascault JP. Die Angew Makromol Chem 1995;13:230.
[32] Lange J, Ekelof R, George GA. Polymer 1999;40(12):3595.
[33] Lange J, Altmann N, Kelly CT, Halley PJ. Polymer 2000;41(15):5949.
[34] Harrani H, Fellahi S, Baker M. J Appl Polym Sci 1999;71:29.
[35] Pearson RA, Yee AF. J Mater Sci 1989;24:2571.
[36] Thomas R, Abraham J, Thomas PS, Thomas S. J Poly Sci Part B Polym Phys 2004;42:2531.
[37] Kinloch AJ, Hunston DL. J Mater Sci Lett 1986;5:909.
[38] Bascom WD, Hunston DL. In: Allex KW, editor. Adhesives, vol. 6. London: Applied Science Publishers; 1980.
[39] Hunston DL, Bascom WD. In: Riew CK, Gillham JK, editors. Rubber modified thermoset resins. Advances in chemistry series no. 208. American Chemical Society; 1984. p. 83–99.
[40] Ratna D. Polymer 2001;42:4209.
[41] Ratna D, Banthia AK, Deb PC. J. Appl Polym Sci 2001;80:1792.
[42] Lanzetta N, Laurienzo P, Malinconico M, Martuscelli E, Ragosta G, Volpe MG. J Mater Sci 1992;27:786.
[43] Chen TK, Jan YH. Polym Eng Sci 1994;34:778.
[44] Kim DS, Kim SC. Polym Eng Sci 1994;34:1598.
[45] De Graaf LA, Hempenious MA, Moller M. Polym Prepr 1995;36:787.
[46] Kinloch AJ, Shaw SJ, Tod DA, Hunston DL. Polymer 1983;24:1355.
[47] Takao I, Naoto Y, Tomoi M. Eur Polym J 1992;28:573.
[48] Manternal S, Pascault JP, Sautereau H. In: Riew CK, editor. Rubber toughened plastics. Advances in chemistry series, vol. 222. Washington, DC: American Chemical Society; 1989. p. 193.
[49] Yee AF, Pearson RA. J Mater Sci 1986;21:2462.
[50] Lee WH, Hodd KA, Hodd WW. In: Riew CK, editor. Rubber toughened plastics. Advances in chemistry series, vol. 222. Washington, DC: American Chemical Society; 1989. p. 263.
[51] Bascom WD, Hunston DL. In: Riew CK, editor. Rubber toughened plastics. Advances in chemistry series, vol. 222. Washington, DC: American Chemical Society; 1989. p. 135.
[52] Eklind H, Maurer FJH. Polym Sci Phys 1996;34:1569.
[53] Eklind H, Maurer FJH. Polymer 1997;38:1047.
[54] Liu YL, Wu CS, Chiu YS, Ho WH. J Polym Sci Polym Chem 2003;41:2354.
[55] Park SJ, Kim HC, Lee HL, Suh DH. Macromolecules 2001;34:7573.
[56] Park SJ, Jin FJ, Lee JR. Macromol Rapid Commun 2004;25:724.
[57] Horowitz HH, Metzger G. Anal Chem 1963;35:1464.